Carbohydrate Polymers 343 (2024) 122504

Contents lists available at ScienceDirect

Carbohydrate Polymers

journal homepage: www.elsevier.com/locate/carbpol

Preparation of superabsorbent composite(s) based on dialdehyde cellulose extracted from banana fiber waste

Boussif Ahmed Yassine [a,b], Mohammed Bezbiz [a,b], Larbi Belachemi [a], Céline Moreau [b], Catherine Garnier [b], Camille Jonchere [b], Hicham Ben youcef [c], Bernard Cathala [b], Hamid Kaddami [a,d,*]

[a] Innovative Materials for Energy and Sustainable Development (IMED-Lab), Cadi Ayyad University, Morocco
[b] UR1268 BIA, INRAE, F-44316 Nantes, France
[c] HTMR, Mohammed VI Polytechnic University, Morocco
[d] SUSMAT-RC, Mohammed VI Polytechnic University, Morocco

ARTICLE INFO

Keywords:
Banana fiber waste
Dialdehyde cellulose
Superabsorbent
Hydrogels
Re-swelling property

ABSTRACT

The study focus is the valorization of banana agriculture by products by the extraction and derivatization of cellulose and its incorporation in formulations to produce superabsorbent materials endowed with high water absorption performances. The extracted cellulose (BP) was subjected to a controlled oxidation by sodium periodate to convert it to cellulose dialdehyde (DAC) with controlled aldehyde content. The cellulosic materials were incorporated into a suspension containing acrylic acid (AA) and itaconic acid (IA) to produce composite hybrid hydrogels (SA-BP/SA-DAC) by radical chain polymerization in water, using *N*,*N*-methylene-bis-acrylamide (MBA) as a cross-linking agent and potassium persulfate (KPS) as an initiator. The prepared materials were characterized using techniques such as Fourier-transform infrared spectroscopy (FTIR), scanning electron microscopy (SEM), and rheological analysis. Additionally, the absorption and re-swelling capacities of the superabsorbent composites (SAPs) were assessed through kinetic studies in water and NaCl solution. Notably, dialdehyde cellulose (DAC), due to its low crystallinity index, hydrophilicity (attributed to aldehyde and hemiacetal functions), and high polarity, holds promise for enhancing the swelling and water retention capacity of the hydrogel. A water absorption capacity as high as 1240±60 g.g-1 was obtained for SA-DAC with a DAC content of 5 %wt. Additionally, the reusability of the SAPs was evidenced.

1. Introduction

Water is a precious natural resource that plays a vital role across the planet (Zheng et al., 2023). The rise in the global human population is leading to a significant rise in the need for water and agricultural products and is generating greater pressure on food production and freshwater resources (Bellù et al., 2018). Today, Morocco as a Mediterranean country has limited water resources and is facing the necessity of reducing water consumption (Zeino-Mahmalat & Bennis, 2012). Water scarcity in Morocco is further accentuated by the effects of climate change, including rising temperatures, the instability and decline of rainfall, and the pressure of agricultural growth (Taheripour et al., 2020). In this context, using superabsorbents to rationalize water use in agriculture is one of the promising solutions.

Superabsorbent polymers (SAPs) are high-performance materials capable of absorbing and retaining water, potentially serving as an excellent water management solution (Jiménez-Rosado et al., 2023). Indeed, water SAPs are hydrophilic three-dimensional networks with the ability to absorb and retain quantities greater than 100 $g.g^{-1}$ of water (Chang et al., 2021; Ostrand et al., 2020). Thanks to their swelling properties, they are employed in various fields such as agriculture, biomedical, and sanitary diapers (Olad et al., 2020). Several investigations have been conducted regarding the agricultural utilization of SAPs (Krasnopeeva et al., 2022). The outcomes have demonstrated notable cost reductions in irrigation, significant improvements in plant survival rates, and a clear enhancement in the retention of fertilizers in the soil (Zhang et al., 2023). However, a predominant portion of the commercially available superabsorbents is synthesized using acrylic acid (AA) or acrylamide (AM) (Chaiyasat et al., 2019; Sawut et al., 2014). These materials have the drawbacks of their high cost, limited

* Corresponding author at: Innovative Materials for Energy and Sustainable Development (IMED-Lab), Cadi Ayyad University, Morocco.
E-mail addresses: bernard.cathala@inrae.fr (B. Cathala), h.kaddami@uca.ma (H. Kaddami).

https://doi.org/10.1016/j.carbpol.2024.122504
Received 24 January 2024; Received in revised form 14 July 2024; Accepted 15 July 2024
Available online 17 July 2024

biodegradability and negative environmental impact (Oladosu et al., 2022).

In contrast, natural polymers have garnered significant attention as potential candidates for fabricating superabsorbents due to their advantages, such as abundance, low cost, biodegradability, and non-toxicity (Li et al., 2023). However, the crucial point of the biobased SAPs reported in the literature, is their lower performances in water absorption when compared to synthetic ones. Jungmin Lee et al. embarked on the synthesis of an SAP hydrogel by blending carboxymethyl cellulose with starch dialdehyde, using citric acid as a cross-linking agent. They obtained an absorption capacity of 87 $g.g^{-1}$ in distilled water (Lee et al., 2018). Cheera Prasad et al. successfully synthesized a superabsorbent polymer (SAP) from carboxymethyl cellulose and starch cross-linked with a biodegradable agent, citric acid (Prasad et al., 2023). They achieved a remarkable absorption capacity of 287 $g.g^{-1}$ in distilled water. Md Nur Alam et al. achieved the synthesis of a bio-SAP using cellulose chitosan cross-linked hydrogels with an absorption capacity of 610 $g.g^{-1}$ in distilled water (Alam & Christopher, 2018). At this stage, hybrid SAPs may provide the opportunity for an ideal balance between absorption-retention capabilities and their environmental impact. Heng-Xiang Li et al. synthesized a hydrogel by grafting cellulose with acrylic acid, using aluminum hydroxide as a cross-linking agent. They achieved an absorption capacity of 922 $g.g^{-1}$ in distilled water (Li et al., 2020). Fang Wu et al. synthesized a hybrid superabsorbent based on cellulose grafted onto a copolymer of acrylic acid and acrylamide, with an absorption capacity of 875 $g.g^{-1}$ in distilled water (Wu et al., 2012). Xiaoxia Li et al. created a hybrid SAP by grafting poly(acrylic acid-*co*-2-acrylamide-2-methyl-1-propanesulfonic acid) onto *Abelmoschus manihot* gum and incorporating microcrystalline cellulose, yielding an even higher absorption capacity of approximately 1240 $g.g^{-1}$ in distilled water (Li et al., 2022). These results show that the hybrid SAPs possess high water absorption capacities compared to the fully biobased SAPs counterparts.

To the best of the authors' knowledge no hybrid SAPs based on DAC has been reported in literature. In view of the chemical structure, morphology and properties of DAC we believe that this cellulose derivative is worthy to be investigated as biobased filler to develop hybrid SAPs with high water absorption capacity and stability. This can also open new opportunities for the use of DACs and agriculture by products valorization.

Banana tree fibers are biomass waste arising from the fibrous residues of pseudostems and leaves that remain after banana culture and harvesting. This agricultural process results in a substantial amount of plant waste material primarily composed of lignocellulosic fibers (Ferdous et al., 2023). Interestingly, the edible fraction, i.e. the fruit itself, contributes to a mere 12 % of the total plant weight (Elanthikkal et al., 2010). The banana plant holds significance as an annual agricultural remnant due to its unique life cycle, yielding fruit only once before being left to decompose in the soil naturally.

This work proposes a new valorization of biomass waste from southern Morocco, in particular waste generated by banana cultivation. The aim is to extract cellulose from these wastes which will be chemically modified and incorporated into new bio-superabsorbent formulations. To this end, the initial phase of this valorization process consists of extracting the cellulose fibers by bleaching treatment to obtain bleached pulp (BP). Subsequently, the extracted cellulose undergoes an oxidation process using sodium periodate to obtain cellulose dialdehydes (DAC) with a controlled aldehyde content (AC). Following this, different composite hybrid hydrogels based on cellulose fibers (BP) or cellulose dialdehydes (DAC) were synthesized by incorporating the cellulose at various fractions into suspensions containing the acrylic acid (AA) and the itaconic acid (IA) as a biobased monomer, followed by radical polymerization in an aqueous medium using *N*, *N*-methylene-bis-acrylamide (MBA) as a cross-linking agent and potassium persulfate (KPS) as an initiator (Bora & Karak, 2022). The characterization of the cellulosic materials (BP and DAC) and the SAP composites (SA-BP and SA-DAC) was conducted using techniques such as Fourier-transform infrared spectroscopy (FTIR), scanning electron microscopy (SEM), and rheological analysis. Absorption and re-swelling capacities of the different SAPs through kinetic studies in water and NaCl solution were assessed. To the authors' knowledge, dialdehyde cellulose (DAC) has rarely been used in the production of water superabsorbent hydrogels. Due to its low crystallinity index, its hydrophilicity coming in particular from the presence of aldehyde and hemiacetal chemical groups, and its high polarity, DAC should improve the swelling and water retention capacity of the hydrogel, for the development of efficient and highly superabsorbent hydrogels.

2. Experimental

2.1. Materials and reagents

Banana tree fibers (BF) were collected from biomass in the south of Morocco. Acrylic acid (AA, 99 %), potassium persulfate (KPS, 99 %), *N*, *N*-methylene-bis (acrylamide) (MBA), sodium hydroxide (NaOH), sodium chlorite ($NaClO_2$), sodium chloride (NaCl), acetic acid (95 %) and ethylene glycol were supplied by Sigma Aldrich. Sodium periodate (99 %) and itaconic acid (IA, 99 %) were purchased from Thermo Fisher Scientific.

2.2. Bleached pulp preparation from Banana fiber

The preparation of bleached pulp (BP) involves the following steps: banana lignocellulosic fibers are ground and sieved to obtain fiber sizes of around 400 μm. These fibers were then alkali-treated with a sodium hydroxide solution (NaOH 3 % *w/v*) for 2 h at 70 °C to remove parts of hemicelluloses and lignin, and this treatment was repeated three times. Then, a second oxidative bleaching treatment was carried out with 1.7 % $NaClO_2$ in a buffer solution (pH = 4.8) containing 27 g NaOH in 500 mL water, 75 mL acetic acid, and 425 mL distilled water, under stirring for 2 h at 70 °C. The protocol was repeated three times. Finally, the bleached cellulose pulp was obtained by repeated filtrations and washing with distilled water (Thien et al., 2022).

2.3. Preparation of dialdehyde cellulose

The preparation procedure of dialdehyde cellulose (DAC) underwent some modifications from that previously described (Ruan et al., 2022). 1 g of bleached banana cellulose pulp suspended in 50 mL of distilled water was introduced into a 100 mL flask covered with aluminum foil (to ensure total darkness of the medium), topped with a reflux condenser, and fitted with a stirring system. The mixture was then sonicated for 30 min in an ultrasonic bath, and the acidity of the mixture was adjusted to pH =3 using acetic acid. Oxidation was carried out using a 0.5 molar equivalent ratio of sodium periodate ($NaIO_4$) to anhydroglucose units (DAC-0.5eq), and the reaction lasted 24 h under magnetic stirring at a temperature of 50 °C. At the end of the reaction, 1 eq of ethylene glycol was added to consume the residual periodate and stop the reaction (1 h at room temperature). Finally, the oxidized cellulose was separated by repeated ultracentrifugations and washings with distilled water. After each centrifugation procedure, the solutions were checked by a Tollens test to detect aldehyde functions. A negative Tollens test indicates that the solutions no longer contain soluble aldehyde oligomers. Finally, the cellulose dialdehydes (DAC) obtained are kept in suspension at a temperature of 4 °C.

2.4. Synthesis of BP/DAC-g-P(AA-co-IA) superabsorbents

SAPs were synthesized using the solution polymerization method. The process involved grafting AA and IA onto the accessible surface chains of BP or DAC. The polymerization was carried out using KPS as the initiator and MBA as a cross-linker (Bora & Karak, 2022). To assess

the impact of various reagents on the resulting SAPs, an optimization was conducted on the amounts of cross-linker MBA, the initiator KPS, the AA to IA ratio, and the degree of AA neutralization.

Initially, the carboxylate groups' fraction of AA was adjusted to 30 % with sodium hydroxide (NaOH). Then, IA was added to 10 mL of distilled water in a 100 mL three-neck round-bottom flask equipped with a mechanical stirrer under a nitrogen atmosphere. The mixture was heated to 85 °C while constantly stirring. Subsequently, a defined amount of BP/DAC suspension was added to the mixture. Following this, the crosslinker MBA and the initiator KPS were added, sequentially. The polymerization reaction was carried out by stirring the resulting mixture for the required time duration at 85 °C. The hydrogels were washed with pure ethanol once the reaction was completed and then air-dried at 60 °C until a stable mass was achieved before being used in further research. The sample codes are designated by 'SA' which refers to the copolymer (AA-IA), followed with the termination 'BPx%' or 'DACx%', with 'x' indicating the percentage of added bleached pulp or cellulose dialdehydes (Table 3). (See Fig. 1.)

2.5. Fourier transform infra-red (FTIR) spectroscopy

The FTIR spectra were recorded using a Perkin Elmer Spectrum 100 FTIR Spectrometer with a resolution of 4 cm^{-1} (16 scans) in the wavenumber range of 450 to 4000 cm^{-1}. The samples were examined as pellets made from 2 mg of the substance combined with 198 mg of KBr for analysis.

2.6. X-ray diffraction (XRD)

The obtained BP and DACs underwent XRD analyses using a Rigaku SmartLab diffractometer, utilizing copper Kα radiation (λ ≃ 1.54 Å). The scanning speed was set at 5°/min, and the range of the 2Θ angle explored was from 2° to 50°. The crystallinity index (Ic) of the cellulose particles was computed using the Segal method, which can be calculated using the following equation (Eq. (1)):

$$I_C = \frac{I_t - I_a}{I_t} \times 100\% \quad (1)$$

Where I_t is the total intensity of the (200) peak for cellulose at 22.7° 2θ, and I_a is the amorphous intensity at 18° 2θ for cellulose and at 16° 2θ for cellulose II.

2.7. Scanning electron microscopy (SEM) analysis

A field emission gun scanning electron microscope (Quattro S, Thermo Fischer Scientific) was used to capture images of the SAPs. The samples were affixed to a metal stub using conductive carbon tape, coated with a 5 nm layer of platinum using an ion-sputter coater (LEICA EM ACE600, Germany), and then examined in HI-VAC mode with a probe current of 30 A at a 5 kV acceleration.

2.8. Rheological characterization of SAPs

Rheological measurements were conducted using an ARES (TA Instruments) controlled strain rheometer equipped with a 40 mm plate-and-plate geometry. The gaps used were selected based on the resistance of gels during manipulations, and the details are presented in Table 1. All experiments were carried out at a temperature of 20 °C. To prevent the samples from evaporating during the measurement process, a layer of paraffin oil was applied. Rheological tests involved the exploration of the storage modulus (G') and loss modulus (G") of the synthesized SAPs over a frequency range extending from 0.001 to 100 rad s^{-1} (frequency sweep experiments). The strains employed were

Table 1
The value of the gap for each SAP.

Sample Name	SA	SA-BP1%	SA-BP5%	SA-DAC1%	SA-DAC3%	SA-DAC4%	SA-DAC5%
Gap (mm)	0.5	1.6	1.3	1.2	1	0.5	0.5

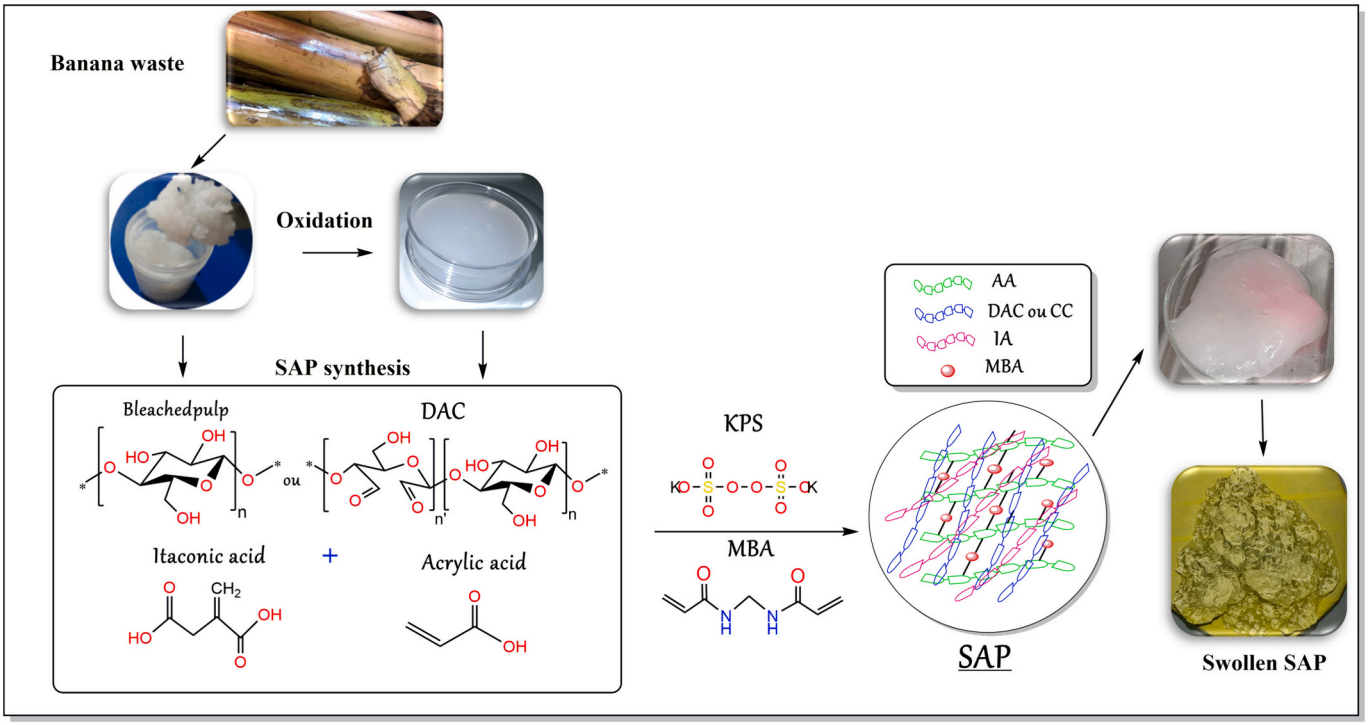

Fig. 1. Synthetic scheme of SAPs preparation from banana biomass.

deliberately selected to operate within the linear viscoelastic (LVE) range, ensuring that G' and G" remain independent of the amplitude of the applied strain.

2.9. Determination of aldehyde content

The aldehyde content was determined using the hydroxylamine hydrochloride (NH_2OH-HCl) oximation method (Kim et al., 2004). Following the quantitative reaction between carbonyl groups and hydroxylamine hydrochloride, the generated hydrochloric acid was titrated using a pH-meter method. Specifically, 0.1 g of oxidized cellulose (DAC) was combined with 25 mL of a hydroxylamine hydrochloride solution (0.2 M), subjected to 30 min of sonication, stirred, and then heated at $T = 40$ °C for 18 h. To halt the reaction, the mixture was cooled by immersion in a cold-water bath upon completion of the designated time. Subsequently, a sodium hydroxide solution (NaOH, 0.2 M) was employed to titrate the generated hydrochloric acid (oxime). The aldehyde content (AC) was calculated using Eq. (2) and confirmed using elementary analysis.

$$AC(\text{mmol}/g) = \frac{C_{NaOH} \times (V_{DAC} - V_{BP})}{m_d} \quad (2)$$

where AC is the aldehyde content of cellulose (mmol/g cellulose), C_{NaOH} is the concentration of sodium hydroxide solution required for titration, V_{DAC} is the equivalence volume with oxidized bleached pulp, V_{BP} is the equivalence volume with unoxidized bleached pulp and m_d is the weight of dry cellulose initially dissolved.

2.10. Elemental analysis

The aldehyde content was determined using the oximation method with hydroxylamine hydrochloride, as described previously (Section 2.9). The results of this method were confirmed by the calculation of the nitrogen content of oximed DAC using an elemental analyzer, specifically the Flash 2000 organic elemental (CHNS) analyzer.

2.11. Measurement of absorption capacity of SAPs

The tea bag method was employed to determine the kinetic as well as the maximum water swelling capacity (Q_m) of the synthesized SAPs (Lu et al., 2015). A specific quantity of dried SAPs was placed inside a tea bag and weighed (m_0). The tea bag was then soaked in water or saline solution (at 0.9 wt%) at 25 °C for a duration of time (t) until swelling equilibrium was reached; at this point, the swollen sample was weighed (m_t). To serve as a control, an experiment was conducted using an empty tea bag. The water absorption capacity at equilibrium (Q_{eq}) of the SAPs was subsequently calculated by considering the difference in weight before and after submersion in water and no further increase of the mass is observed, as outlined in Eq. (3).

$$Q_{eq}(g/g) = (m_t - m_0)/m_0 \quad (3)$$

where m_0 and m_t are the weights of the dried and swollen samples, respectively.

2.12. Re-swelling tests

Dry SAPs were precisely weighed, submerged in distilled water at 25 °C until swelling equilibrium was reached, removed, and weighed again as described in section (3.10). Q_{eq} was then computed using Eq. (3). After drying the swelled sample to constant weight in an oven at 50 °C, the procedure was repeated three times.

3. Results and discussion

SAPs were synthesized using a conventional free radical polymerization process with AA, IA as monomers, DAC/BP as filler, KPS as the initiator, and MBA as the crosslinker. An aqueous medium was employed to prepare SAPs. The process consisted of three steps: initiation, where sulfate anion radicals were produced; chain propagation, where macroradicals initiated grafting copolymerization; and termination, involving deprotonation or combination of living polymeric chains. This method resulted in the formation of a 3D cross-linked network structure for the SAPs (Gharekhani et al., 2017; Olad et al., 2018).

3.1. Characterization of bleached pulp and DAC

To prove the efficiency of the oxidation of bleached cellulose pulp by sodium periodate, and to ensure that the desired DACs were obtained, analyses by FTIR spectroscopy and X-ray diffraction were performed (Fig. 2 a and b).

From FTIR spectra, BP shows a broad band at around 3420 cm^{-1}, and a band at 1640 cm^{-1} corresponding to the stretching and bending vibration bands of OH hydroxyls (Qian et al., 2019). This is followed by a band at 2910 cm^{-1} corresponding to the C-H stretching vibration, as well as a band at 1057 cm^{-1} which is attributed to the C-O-C linkage of cellulose (Huang et al., 2020). Bands between 1420 cm^{-1} and 1320 cm^{-1} are attributed to C-H shear and -OH bending vibrations (Kimani et al., 2016). The DAC-0.5eq spectra shows the same fingerprint as the bleached pulp, with the same characteristic bands except for the additional bands at 1730 cm^{-1}, which is attributed to the vibration of the aldehyde carbonyl of the DAC (Aitbella et al., 2024), and that at 880 cm^{-1} which is characteristic of hemiacetal groups formed between aldehyde functions and alcohols. Other additional but less significant changes on the bands at 2900 cm^{-1} and 1050 cm^{-1} for deformation and vibration of -CH_2 and elongation vibrations of C-O-C were also observed.

To assess the effect of the oxidation on the crystallinity of DAC, the original (BP) and the oxidized pulp with 0.5 eq of sodium periodate were examined by X-ray diffraction (Fig. 2b). The characteristic peaks of cellulose-I at $2\theta = 16.3°$ and $2\theta = 22.5°$ are clearly observable for the two samples (Zhang et al., 2018). However, the crystallinity index decreases from 65 % to 44 % for BP and pulp treated with 0.5 equivalent of DAC (DAC-0.5eq), respectively (Table 2). The oxidation process affects the amorphous regions and progressively affects the crystalline region of cellulose by breaking C_2-C_3 bonds and consequently leads to a significant decrease in the crystallinity degree.

To evaluate the effect of the oxidation on the cellulose fibers structure, morphological analyses of the fibers of BP and DAC-0.5eq were conducted (Fig. 2c). As observed in Fig. 2c (i, ii), The bleached cellulosic pulp (BP) has a fibrous structure, featuring both rough and smooth surfaces, with a diameter of approximately 10 ± 2 μm. On the contrary, the morphology of the oxidized DACs (Fig. 2c (iii, iv)) undergoes a gradual transformation into microfibrils, leading to a noticeable decrease in fiber diameter to approximately 6 ± 1 μm giving evidence of a degradation process (Li et al., 2011).

The quantification of the aldehyde content (AC) resulting from the oxidation reaction of bleached pulp by sodium periodate was established by the method of oximation of the DAC using the equation (Eq. (2)) and this is confirmed by the elemental nitrogen analysis. The results, presented in Table 2, show that DAC-0.5eq exhibits an aldehyde content of 3.3 mmol/g. On the other, the strength of the degrading effect of the oxidative process is evaluated by the mass yield of cellulose after oxidation. The results show a degradation percentage of 33 % in the reaction conditions used.

3.2. SAPs preparation and characterization

Table 3 comprises all prepared SAPs with different reagent compositions. A water-based medium was employed for SAPs preparation by mean of radical polymerization. The prepared SAPs were characterized by FTIR to have an insight on their chemical structure. Subsequently, morphological analyses were performed using SEM to visualize the

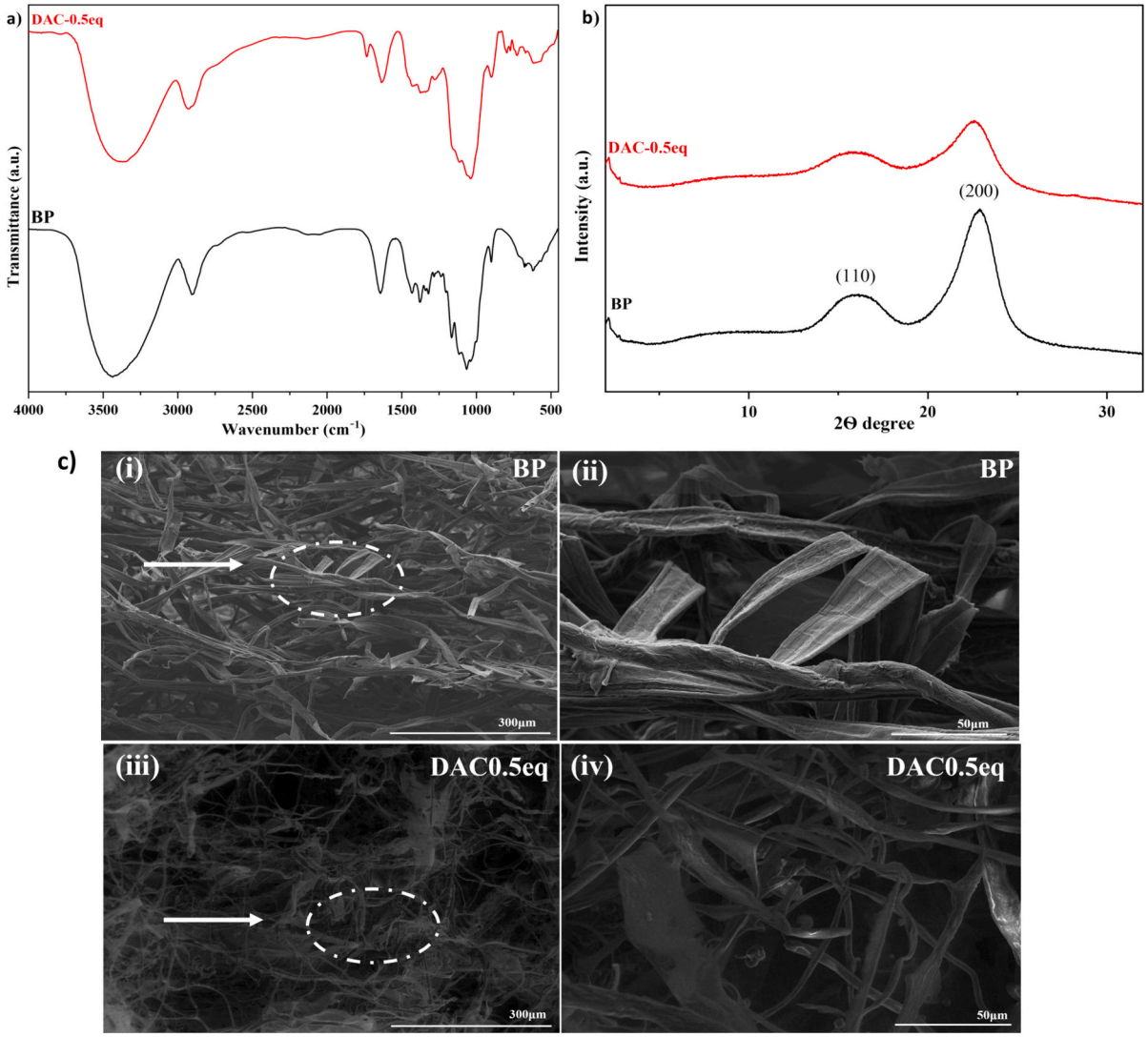

Fig. 2. (a) FTIR spectra and (b) XRD spectra of bleached pulp (BP), and DAC-0.5eq, (c) SEM images of the bleached pulp (i, ii) and DAC-0.5 (iii, iv).

Table 2
Aldehyde content (AC), degradation percentage, and crystallinity percentage of oxidized bleached pulp.

Periodate Equivalent	AC (mmol/g) ±0.1	Degradation (%)	Crystallinity (%)
0	–	–	65
0.5	3.3	33	44

Table 3
Composition (wt%) of the different prepared SAPs.

Sample name	AA/MBA	IA	BP	DAC-0.5eq
SA	85 (84.5/0.5)	15	–	–
SA-BP1%	84 (83.5/0.5)	15	1	–
SA-BP5%	80 (79.5/0.5)	15	5	–
SA-DAC1%	84 (84.5/0.5)	15	–	1
SA-DAC3%	82 (81.5/0.5)	15	–	3
SA-DAC4%	81 (80.5/0.5)	15	–	4
SA-DAC5%	80 (79.5/0.5)	15	–	5
SA-DAC7.5%	77.5 (77/0.5)	15	–	7.5

incorporation of fibers and porosity in the hydrogel structure. Rheological analyses were also conducted to investigate the effect of BP and DAC on the hydrogel mechanical strength. Finally, investigations of the absorption capacities and reusability of the SAPs were carried out.

3.2.1. FTIR analysis

FTIR analysis was conducted to examine the process of grafting acrylic acid (AA) and itaconic acid (IA) onto the backbone of BP and DAC (Fig. 3).

As for BP and DAC (Fig. 2a), the FTIR spectra of, AA, IA, and SAPs reveal a broad band in the range 3300–3400 cm^{-1} indicating the presence of bands related to hydroxyl (OH). Smaller and narrower bands around 2850 and 2920 cm^{-1} are observed for SA samples and are attributed to the vibration of symmetric and asymmetric stretching of CH_2 groups. In addition, the strong bands around 1720 cm^{-1} correspond to the elongation vibration of the carboxylic carbonyl groups that are overlapping with the N-H bending vibration band of the cross-linking agent in the structure of SAPs. On the other hand, the bands around 1560 cm^{-1} are due to the stretching vibration of the carboxylate groups. The bands in the domain 1620–1650 cm^{-1} in the AA and IA spectra correspond to C=C double bands. The intensities of these bands decrease significantly in the SAPs, and almost disappear in the spectra of SA-BP5% and SA-DAC5%. Al these observations indicate that the SAPs were successfully synthesized.

3.2.2. SEM analysis

The surface morphology of the synthesized superabsorbent (SAPs) (i.

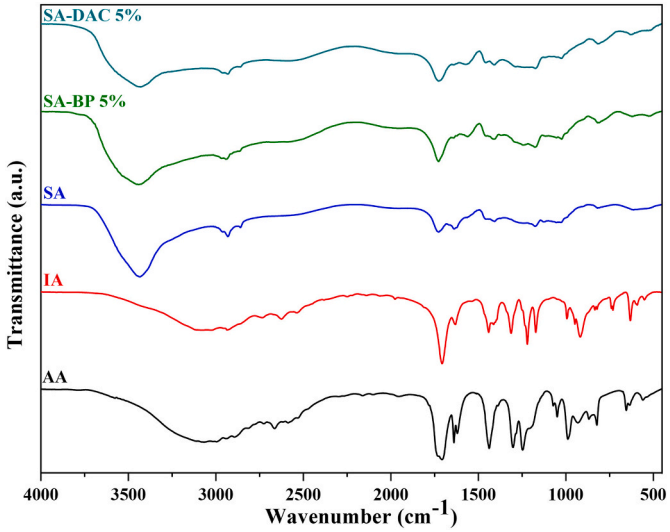

Fig. 3. Infrared spectra of the reagents AA, IA, and the synthesized superabsorbent polymers SA, SA-BP 5 %, and SA-DAC 5 %.

e., DAC copolymer and/or bleached pulp-co-(acrylic acid-co-itaconic acid) (SA-BP 5 % and SA-DAC 5 %)) was examined using a scanning electron microscope (SEM) (Fig. 4). It can be observed that the SAPs exhibit smooth microstructures with closed pores of various sizes and relief features, along with the appearance of dispersed cellulose fibrils on the surface. The association between the fibers and the polymer is strong and no detachment of the fiber is observed.

3.2.3. Rheology measurements

To study the mechanical properties of the network of synthesized SAPs, G', storage modulus, and G", loss modulus, were recorded in the angular frequency range of 0.001 to 100 rad s^{-1}. As shown in Fig. 5 (a, b), for all the samples, G' consistently exceeds G" throughout the entire frequency range, evidencing the predominance of elastic behavior in all the systems (Mohammadbagheri et al., 2021). For SA hydrogel, both G' and G" increased with the frequency, leading to a crossover between G' and G" at the highest frequencies, displaying the existence of relaxation time of the order of the period of the mechanical strain imposed (inverse of frequencies). The incorporation of bleached pulp, at 1 % and 5 % (SA-BP1,5 %) concentration, enhances the hydrogel mechanical properties, with higher values of G' and G", less frequency dependency, and lower loss factors (tan δ). No crossover between G' and G" is observed in the presence of BP, G' being over G" at the highest frequency, showing a better structuration. Subsequently, the addition of DAC (Fig. 5b) demonstrates a significant increase in gel strength at 1 %, followed by a subsequent decrease compared to the addition of 3 %. Similarly, at 4 % and 5 %, the properties remain almost identical to those of SA. Additionally, it is observed that hydrogels prepared with DAC exhibit higher slopes than those prepared with BP. Furthermore, in contrast to SAPs with BP, SA-DAC shows crossing points between G' and G", suggesting different structuring mechanisms between BP and DAC. The introduction of cellulose fibers at a 5 % rate notably enhances the mechanical properties of SA-BP hydrogel (Etminani-Isfahani et al., 2020). Conversely, the inclusion of DACs does not result in any substantial variance in mechanical characteristics.

3.3. Swelling properties of superabsorbents

3.3.1. Absorption capacity of SAPs

To determine the impact of the BP and DACs in SAPs on the absorption capacities of the different samples, kinetic studies of swelling capacity in distilled water (Fig. 6a) and in saline solution (0.9 % *w/v* NaCl) (Fig. 6b) were carried out using the "tea-bag method" (Zhang et al., 2020).

All SAPs exhibit two different kinetic phases in distilled water. A first phase during which water molecules diffuse rapidly into the pores over the first five hours. This is followed by a second phase of slower water diffusion, during which water molecules infiltrate the more confined spaces and the new spaces created by initial swelling and electrostatic repulsions. This second phase extends until equilibrium. The equilibriums were reached at different times for the different SAPs, with all of them reaching this state almost after thirty hours of immersion.

The immersion of SAPs in the saline solution demonstrated lower

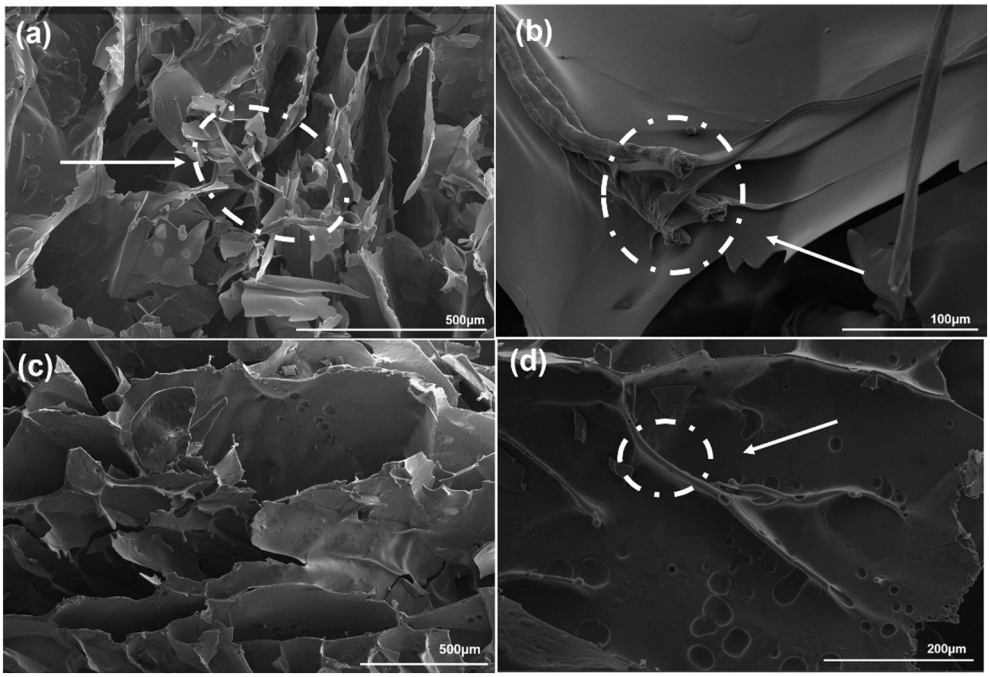

Fig. 4. SEM images of SA-BP 5 % ((a) 500 µm, (b) 100 µm) and SA-DAC 5 % ((c) 500 µm, (d) 200 µm).

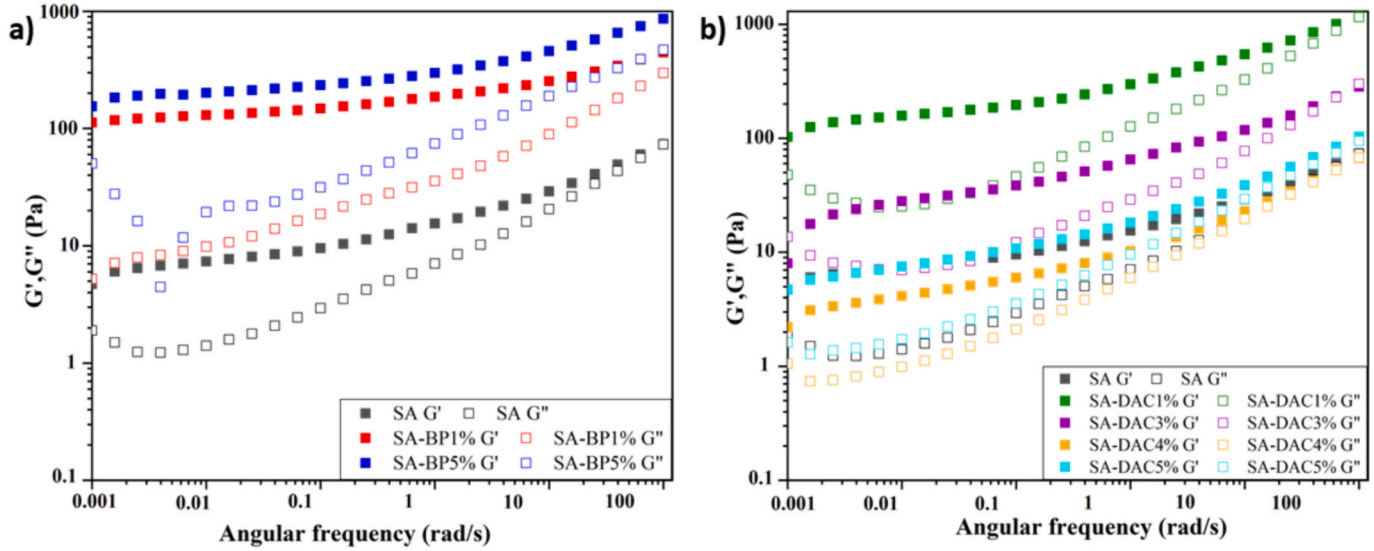

Fig. 5. Frequency dependence of storage modulus (G) and loss modulus (G') at a constant strain, a) SAPs with the incorporation of BP, b) with the incorporation of DAC-0.5eq.

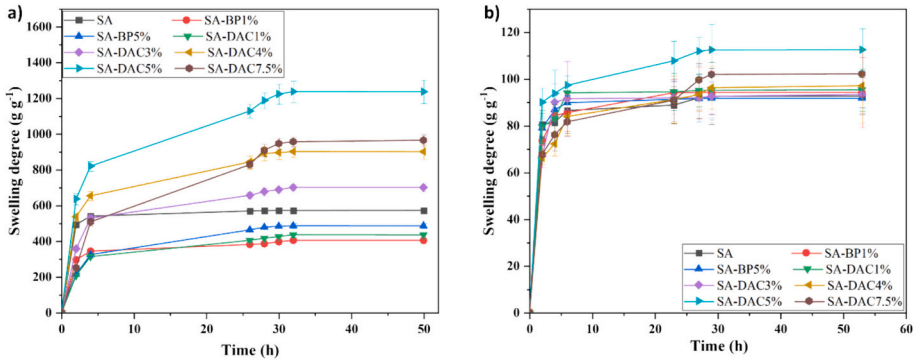

Fig. 6. Kinetic absorption curves of SAPs in (a) distilled water and (b) 0.9 wt% NaCl as a function of time.

water absorption, primarily occurring during the first phase, followed by a slight increase during the second phase until reaching equilibrium. It is worth noting that there the tenfold difference between the water absorption capacities in distilled water and that in a 0.9 % NaCl solution is due to the ionic forces generated by the saline solution. The presence of Na^+ and Cl^- ions in this solution could produce the screening effect, which would block the influence of electrostatic repulsions by protecting the carboxylate anions of the polymer chains. This screening effect might promote the establishment of new physical interactions, such hydrogen bonds, which make the network more resistant to the osmotic pressure and leads to a reduction in water absorption capacity.

In distilled water, the addition of BP to the SAPs formulation decreases the absorption capacity compared to that of SA (570 $g.g^{-1}$). However, at 1 % BP, a value of 404 $g.g^{-1}$ is observed for SA-BP1%, which increases with the increase in BP percentage, reaching 485 $g.g^{-1}$ for SA-BP5%. Similarly, the incorporation of DACs at 1 % reduces the absorption capacity with SA-DAC1% (435 $g.g^{-1}$), but this capacity increases significantly with the increase in DACs percentage: SA-DAC3% (700 $g.g^{-1}$), SA-DAC4% (901 $g.g^{-1}$), reaching the maximum value for SA-DAC5% (1240 $g.g^{-1}$), and then decreasing to 960 $g.g^{-1}$ for SA-DAC7.5 %. In saline solution, all SAPs exhibit an absorption capacity of about 90 $g.g^{-1}$, except for SA-DAC5%, which displays a capacity of 112 $g.g^{-1}$, and SA-DAC7.5 %, which reaches 102 $g.g^{-1}$. In conclusion, SAPs based on cellulose dialdehydes exhibited significantly higher absorption capacity performances compared to those based on bleached pulp.

According to Etminani-Isfahani et al., water absorption occurs through water diffusion in free spaces following a Fickian kinetics similar to the synthetic SAPs of neat polyacrylate (without DAC) (Etminani-Isfahani et al., 2020). The entanglements of the polyacrylate chain interactions between polyacrylate chains and the cellulose fibers of DACs slow down the mobility of water molecules during this phase. Furthermore, As reported by Dai et al., the water absorption in these systems follows a pseudo-second-order kinetic model describing the swelling as diffusion of water molecules through the polymeric chains and by mean of pores (Dai & Huang, 2017). In our case, we believe that DAC increases the porosity inside the SAP and consequently contributes to improving water absorption capacity, but does not modify significantly the kinetic because of the low fraction of DAC used (5 wt%).

3.3.2. *Reswelling ability of SAPs*

To assess the reusability of synthesized SAPs, an absorption-desorption study in distilled water was conducted. Their equilibrium absorption capacity and their stability after three successive dry-wet cycles were evaluated (Fig. 7).

The SAPs show an average absorption capacity of around 80 % of the initial capacity after the third absorption-desorption cycle, except for SA-DAC 5 %, which decreased from 1240 to 832 $g.g^{-1}$, representing around 67 % of its initial capacity. This result is similar to those described by **Xie Ye** (Ye et al., 2021) using hydroxypropyl methyl cellulose with the same number of cycles. Indeed, this drop in swelling

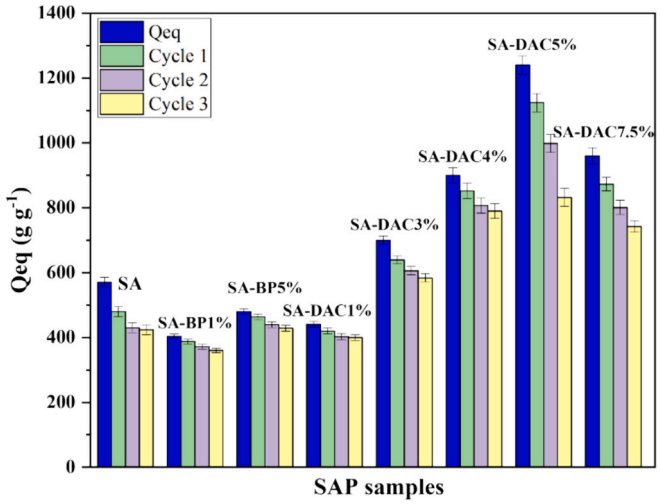

Fig. 7. Reusability tests in distilled water of different synthesized superabsorbents.

capacity can be interpreted by two possible explanations: the first relates to a slight loss of mass after the water immersion operation, which can be explained by a partial detachment and solubilization of aldehydic oligomers and/or polyacrylic oligomers trapped in the network and released during swelling. The second concerns a possible reduction in free spaces with a decrease in flexibility during drying steeps at 50 °C, with a collapse of the pores. There are fewer opportunities for hydrogen bonding, as drying by eliminating water molecules irreversibly removes some of the bonding sites (Alam & Christopher, 2018). In addition to these possible phenomena, the drying of BioSAPs between consecutive cycles at 50 °C in an oven might induce an interfibril hornification of DAC that contributes to reducing the water sorption (Santmarti et al., 2020), as well as cross-links between the macromolecular chains which is favored by the formation of hemiacetals from aldehyde functions and primary alcohols (inter-chain hemiacetal formation C-2/C-6 and C-3/C-6, chain cross-linking), which would cause a partial irreversible closure of certain pores and limit swelling (Mo et al., 2022).

3.4. Discussion

Banana fiber waste derived cellulose, along with cellulose dialdehydes, were successfully employed in combination with itaconic acid as a biobased acid, acrylic acid, potassium persulfate as an initiator, and *N*, *N*-methylene bisacrylamide as a crosslinker to synthesized hybrid superabsorbents.

FTIR results revealed characteristic bands of superabsorbent polymers (SAPs), confirming the successful grafting of acrylic monomers onto BP/DAC chains. SEM images depicted cellulose fibrils between and on the surface of the (AA-co-IA) copolymer, indicating a porous structure of the hydrogels as well as a strong interaction between fibers and polymer. Rheological analysis revealed that the addition of BP contributed to improving the mechanical properties of hydrogels. In contrast, the incorporation of DAC did not result in a significant mechanical reinforcement. DAC exhibits a less crystalline structure than BP, leading to more pronounced fibrillation than BP. This suggests differences between the two fillers in influencing the mechanical properties of the SAP scomposites.

The addition of hydrophilic cellulose dialdehydes (DACs) at a percentage of 5 % enables the formation of new intermolecular hydrogen bonds with poly (acrylic acid) chains, providing greater flexibility and elasticity. This results in a higher swelling capacity in water. SA-DAC5% exhibited a water absorption capacity in distilled water of 1240 g.g^{-1}, significantly higher than that of both the unfilled copolymer, SA (570 g.g^{-1}) and SA- BP 5 % (485 g.g^{-1}) composite, and even higher than that of SA-DAC7.5 % (960 g g^{-1}). This demonstrates that 5 % DAC is the optimal fraction to provide SAPs with the highest water absorption capacity. The low crystallinity and the porous microstructures of the DAC fibers, which adhere well to the polymer matrix, significantly contribute to creating new free spaces that promote the diffusion of water in their network during the swelling process.

The results show that SAPs SA-DAC exhibit higher absorption capacities compared to those of SA-BP, leading to the conclusion that the absorption capacity of the gels is inversely related to the strength (Etminani-Isfahani et al., 2020). The synthesized hybrid SAP, with an absorption capacity of 1240 g.g^{-1}, demonstrates better performance than those reported in the literature for similar hybrid SAPs (Table 4) (Sikder et al., 2021). On the other hand, these hybrid SAPs own favorable performances in comparison to natural-polymer based SAPs. For example, a cellulose-based aerogel crosslinked with citric acid showed a water absorption of 99 g.g^{-1} in DI water (Kaya, 2017). Cellulose nanofibril gel via the ester cross-linking (Li et al., 2018) exhibited water absorbency of 124 g.g^{-1} for water.

4. Conclusion

In summary, biodegradable, inexpensive, and environmentally friendly superabsorbent composite hydrogels, SA-BP and SA-DAC, demonstrating advantageous water absorption capacities, were effectively synthesized by radical chain polymerization in an aqueous medium. The incorporation of 20 % of biobased components (Cellulosic filler and IA monomer) in these new hybrid SAP provide a significant benefit in terms of swelling in water, improvement of their biodegradability, their low cost, ecological sustainability, as well as the reduction of their toxicity. The swelling abilities of the absorbents from all-natural products are usually lower than the ones containing partly synthetic materials. The water absorption and swelling mechanisms of the synthesized SA-DAC superabsorbent hydrogels involve several key parameters. Firstly, the copolymerization of acrylic acid and itaconic acid leads to a material carrying several negatively charged carboxylate functions which causes repulsive forces between the macromolecular chains and consequently, creates spaces that promote the water mobility in networks in the copolymer network. In addition, the incorporation of highly amorphous and porous dialdehyde cellulose which is significantly hydrophilic and capable of creating new hydrogen bonds between water and aldehyde and hemiacetal functions on the surface of the DAC increases the swelling capacity of the SAP and improves the flexibility of the networks. The combination of all these parameters gives these Biobased Superabsorbents a remarkable swelling capacity in water and appear as promising environmentally friendly agricultural superabsorbent candidates for the storage and saving of water and its controlled retention in the soil. This makes it capable to act as an active agent carrier and soil conditioner. Finally, despite the enormous absorption capacities provided by hybrid and synthetic systems, we are attempting, in the ongoing study, to prepare entirely bio-sourced SAPs with high

Table 4
Comparison of the capacity performance of SA-DAC5% to those reported in the literature.

Type of polymer	Swelling/Water (g g^{-1})	References
Poly (acrylic acid)	407	(Cruz et al., 2020)
Hydroxy ethyl cellulose-co-acrylamide	1220	(Ghobashy et al., 2023)
Sodium alginate-g-Poly(acrylic-*co*-acrylamide)/modified diatomite	505	(Wang et al., 2024)
poly (acrylic acid) – graft – chitosan	715	(Barleany et al., 2017)
(chitosan-alginate)-g-poly (acrylic acide)	941	(Medha & Sethi, 2024)
DAC-g-Poly (acrylic-*co*-itaconic acide)	1240	this work

performance based on a blend of cellulose and other biobased polymers.

CRediT authorship contribution statement

Boussif Ahmed Yassine: Writing – original draft, Investigation. **Mohammed Bezbiz:** Investigation, Formal analysis. **Larbi Belachemi:** Writing – review & editing, Supervision, Conceptualization. **Céline Moreau:** Writing – review & editing, Supervision. **Catherine Garnier:** Writing – review & editing, Investigation. **Camille Jonchere:** Writing – review & editing, Investigation. **Hicham Ben youcef:** Writing – review & editing, Project administration. **Bernard Cathala:** Writing – review & editing, Supervision, Conceptualization. **Hamid Kaddami:** Writing – review & editing, Supervision, Methodology, Funding acquisition, Conceptualization.

Declaration of competing interest

The authors declare that they have no known competing financial interest.

Data availability

No data was used for the research described in the article.

Acknowledgment

The authors gratefully acknowledge the UM6P, The CNRST & the "Ministère de l'Enseignement Supérieur de la Recherche et de l'Innovation of Morocco" for the financial support through the research program APRD under the agreement APRD 25153, Project name "BIOSAP".

Appendix A. Supplementary data

Supplementary data to this article can be found online at https://doi.org/10.1016/j.carbpol.2024.122504.

References

Aitbella, H., Belachemi, L., Merle, N., Zinck, P., & Kaddami, H. (2024). Schiff Base functionalized cellulose: Towards strong support-cobalt nanoparticles interactions for high catalytic performances. *Molecules, 29*(8), 1734.

Alam, M. N., & Christopher, L. P. (2018). Natural cellulose-chitosan cross-linked superabsorbent hydrogels with superior swelling properties. *ACS Sustainable Chemistry & Engineering, 6*(7), 8736–8742.

Barleany, D. R., Dhamar Lestari, R. S., Yulvianti, M., Susanto, T. R., & Shalina, -, & Erizal, -.. (2017). Acrylic acid neutralization for enhancing the production of grafted chitosan superabsorbent hydrogel. *International Journal on Advanced Science, Engineering and Information Technology, 7*(2), 702.

Bellù, L. G., Kavallari, K., Müller, M., & Nguyen, L. H. (2018). *FAO, IFAD, the future of food and agriculture – Alternative pathways to 2050*. Summary version. Rome. 60 pp.

Bora, A., & Karak, N. (2022). Starch and itaconic acid-based superabsorbent hydrogels for agricultural application. *European Polymer Journal, 176*, Article 111430.

Chaiyasat, A., Jearanai, S., Christopher, L. P., & Alam, M. N. (2019). Novel superabsorbent materials from bacterial cellulose: Novel superabsorbent materials from bacterial cellulose. *Polymer International, 68*(1), 102–109.

Chang, L., Xu, L., Liu, Y., & Qiu, D. (2021). Superabsorbent polymers used for agricultural water retention. *Polymer Testing, 94*, Article 107021.

Cruz, H., Laycock, B., Strounina, E., Seviour, T., Oehmen, A., & Pikaar, I. (2020). Modified poly(acrylic acid)-based hydrogels for enhanced mainstream removal of ammonium from domestic wastewater. *Environmental Science & Technology, 54*(15), 9573–9583.

Dai, H., & Huang, H. (2017). Enhanced swelling and responsive properties of pineapple Peel Carboxymethyl cellulose- *g* -poly(acrylic acid- *co* -acrylamide) superabsorbent hydrogel by the introduction of carclazyte. *Journal of Agricultural and Food Chemistry, 65*(3), 565–574.

Elanthikkal, S., Gopalakrishnapanicker, U., Varghese, S., & Guthrie, J. T. (2010). Cellulose microfibres produced from banana plant wastes: Isolation and characterization. *Carbohydrate Polymers, 80*(3), 852–859.

Etminani-Isfahani, N., Mohammadbagheri, Z., & Rahmati, A. (2020). 4-(6-Aminohexyl) amino-4-oxo-2-butenoic acid as a novel hydrophilic monomer for synthesis of cellulose-based superabsorbents with high water absorption capacity. *Carbohydrate Polymers, 250*, Article 116959.

Ferdous, T., Quaiyyum, M. A., Jin, Y., Bashar, M. S., Yasin Arafat, K. M., & Jahan, M. S. (2023). Pulping and bleaching potential of banana pseudo stem, banana leaf and banana peduncle. *Biomass Conversion and Biorefinery, 13*(2), 893–904.

Gharekhani, H., Olad, A., Mirmohseni, A., & Bybordi, A. (2017). Superabsorbent hydrogel made of NaAlg-g-poly(AA-co-AAm) and rice husk ash: Synthesis, characterization, and swelling kinetic studies. *Carbohydrate Polymers, 168*, 1–13.

Ghobashy, M. M., Amin, M. A., Ismail, M. A., Nowwar, A. I., El-diehy, M. A., & Gayed, H. M. (2023). Radiation cross-linked ultra-absorbent hydrogel to rationalize irrigation water and fertilizer for maize planting in drought conditions. *International Journal of Biological Macromolecules, 252*, Article 126467.

Huang, X., Dognani, G., Hadi, P., Yang, M., Job, A. E., & Hsiao, B. S. (2020). Cationic Dialdehyde Nanocellulose from sugarcane bagasse for efficient chromium(VI) removal. *ACS Sustainable Chemistry & Engineering, 8*(12), 4734–4744.

Jiménez-Rosado, M., Perez-Puyana, V., & Romero, A. (2023). The use of biowaste for the production of biodegradable superabsorbent materials. *Current Opinion in Food Science, 49*, Article 100975.

Kaya, M. (2017). Super absorbent, light, and highly flame retardant cellulose-based aerogel crosslinked with citric acid. *Journal of Applied Polymer Science, 134*(38), Article 45315. https://doi.org/10.1002/app.45315

Kim, U.-J., Wada, M., & Kuga, S. (2004). Solubilization of dialdehyde cellulose by hot water. *Carbohydrate Polymers, 56*(1), 7–10.

Kimani, P., Kareru, P., Madivoli, S., Kairigo, P., Maina, E., & Rechab, O. (2016). Comparative study of carboxymethyl cellulose synthesis from selected Kenyan biomass. *Chemical Science International Journal, 17*(4), 1–8.

Krasnopeeva, E. L., Panova, G. G., & Yakimansky, A. V. (2022). Agricultural applications of superabsorbent polymer hydrogels. *International Journal of Molecular Sciences, 23*(23), Article 15134.

Lee, J., Park, S., Roh, H., Oh, S., Kim, S., Kim, M., … Park, J. (2018). Preparation and characterization of superabsorbent polymers based on starch aldehydes and carboxymethyl cellulose. *Polymers, 10*(6), 605.

Li, H., Wu, B., Mu, C., & Lin, W. (2011). Concomitant degradation in periodate oxidation of carboxymethyl cellulose. *Carbohydrate Polymers, 84*(3), 881–886.

Li, H.-X., Tian, X., Zhang, L., Wang, L., Jin, L., & Cao, Q. (2020). Synthesis and properties of cellulose-based superabsorbent hydrogel by a new crosslinker. *Fibers and Polymers, 21*(7), 1395–1402.

Li, S., Hernandez, S., & Salazar, N. (2023). Biopolymer-based hydrogels for harvesting water from humid air: A review. *Sustainability, 15*(1), 848.

Li, X., Wang, X., Sang, W., Liu, B., Peng, H., Zhang, W., & Ma, G. (2022). Preparation and anti-leakage performances of superabsorbent composite based on ablmoschus manihot gum and microcrystalline cellulose. *Journal of Environmental Chemical Engineering, 10*(3), Article 107644.

Li, Y., Liu, Y., Liu, Y., Lai, W., Huang, F., Ou, A., … Wang, X. (2018). Ester crosslinking enhanced hydrophilic cellulose Nanofibrils aerogel. *ACS Sustainable Chemistry & Engineering, 6*(9), 11979–11988.

Lu, J., Li, Y., Hu, D., Chen, X., Liu, Y., Wang, L., & Zhao, Y. (2015). Synthesis and properties of pH-, thermo-, and salt-sensitive modified poly(aspartic acid)/poly(vinyl alcohol) IPN hydrogel and its drug controlled release. *BioMed Research International, 2015*, 1–12.

Medha, & Sethi, S. (2024). Chitosan based hybrid superabsorbent for controlled drug delivery application. *Biotechnology Progress, 40*(2), Article e3418.

Mo, W., Chen, K., Yang, X., Kong, F., Liu, J., & Li, B. (2022). Elucidating the hornification mechanism of cellulosic fibers during the process of thermal drying. *Carbohydrate Polymers, 289*, Article 119434.

Mohammadbagheri, Z., Rahmati, A., & Hoshyarmanesh, P. (2021). Synthesis of a novel superabsorbent with slow-release urea fertilizer using modified cellulose as a grafting agent and flexible copolymer. *International Journal of Biological Macromolecules, 182*, 1893–1905.

Olad, A., Doustdar, F., & Gharekhani, H. (2020). Fabrication and characterization of a starch-based superabsorbent hydrogel composite reinforced with cellulose nanocrystals from potato peel waste. *Colloids and Surfaces A: Physicochemical and Engineering Aspects, 601*, Article 124962.

Olad, A., Gharekhani, H., Mirmohseni, A., & Bybordi, A. (2018). Superabsorbent nanocomposite based on maize bran with integration of water-retaining and slow-release NPK fertilizer. *Advances in Polymer Technology, 37*(6), 1682–1694.

Oladosu, Y., Rafii, M. Y., Arolu, F., Chukwu, S. C., Salisu, M. A., Fagbohun, I. K., … Haliru, B. S. (2022). Superabsorbent polymer hydrogels for sustainable agriculture: A review. *Horticulturae, 8*(7), 605.

Ostrand, M. S., DeSutter, T. M., Daigh, A. L. M., Limb, R. F., & Steele, D. D. (2020). Superabsorbent polymer characteristics, properties, and applications. *Agrosystems, Geosciences & Environment, 3*(1), Article e20074.

Prasad, C., Park, S. Y., Lee, J. S., Park, J. J., Jang, Y., Lee, S. W., … Choi, H. Y. (2023). Modeling and investigation of swelling kinetics of sodium carboxymethyl cellulose/starch/citric acid superabsorbent polymer. *International Journal of Biological Macromolecules, 253*, Article 127013.

Qian, L., Yang, M., Chen, H., Xu, Y., Zhang, S., Zhou, Q., He, B., Bai, Y., & Song, W. (2019). Preparation of a poly(ionic liquid)-functionalized cellulose aerogel and its application in protein enrichment and separation. *Carbohydrate Polymers, 218*, 154–162.

Ruan, C.-Q., Kang, X., & Zeng, K. (2022). Preparation of water-soluble dialdehyde cellulose enhanced chitosan coating and its application on the preservation of mandarin fruit. *International Journal of Biological Macromolecules, 203*, 184–194.

Santmarti, A., Tammelin, T., & Lee, K.-Y. (2020). Prevention of interfibril hornification by replacing water in nanocellulose gel with low molecular weight liquid poly (ethylene glycol). *Carbohydrate Polymers, 250*, Article 116870.

Sawut, A., Yimit, M., Sun, W., & Nurulla, I. (2014). Photopolymerisation and characterization of maleylatedcellulose-g-poly(acrylic acid) superabsorbent polymer. *Carbohydrate Polymers, 101*, 231–239.

Sikder, A., Pearce, A. K., Parkinson, S. J., Napier, R., & O'Reilly, R. K. (2021). Recent trends in advanced polymer materials in agriculture related applications. *ACS Applied Polymer Materials, 3*(3), 1203–1217.

Taheripour, F., Tyner, W. E., Haqiqi, I., & Sajedinia, E. (2020). *Water scarcity in Morocco: Analysis of key water challenges*. Washington, DC: World Bank.

Thien, D. V. H., Lam, D.-N., Diem, H. N., Pham, T. Y. N., Bui, N. Q., Truc, T. N. T., & Van-Pham, D.-T. (2022). Synthesis of cellulose-g-poly(acrylic acid) with high water absorbency using pineapple-leaf extracted cellulose fibers. *Carbohydrate Polymers, 288*, Article 119421.

Wang, Y., Fu, E., Saghir, S., & Xiao, Z. (2024). Novel superabsorbent polymer composite embedded with sodium alginate and diatomite for excellent water absorbency, water retention capacity, and high thermal stability. *Journal of Molecular Structure, 1300*, Article 137244.

Wu, F., Zhang, Y., Liu, L., & Yao, J. (2012). Synthesis and characterization of a novel cellulose-g-poly(acrylic acid-co-acrylamide) superabsorbent composite based on flax yarn waste. *Carbohydrate Polymers, 87*(4), 2519–2525.

Ye, X., Peng, H., Liu, X., Xiong, H., Wang, N., Yang, F., Kong, Y., Yang, Z., & Lei, Z. (2021). Preparation and fertilizer retention/anti-leakage performances of superabsorbent composite based on hydroxypropyl methyl cellulose. *Carbohydrate Polymers, 274*, Article 118636.

Zeino-Mahmalat, E., & Bennis, A. (2012). *Environnement et Changement Climatique au Maroc Diagnostic et Perspectives*. Konrad-Adenauer-Stiftung e.V.

Zhang, K., Feng, W., & Jin, C. (2020). Protocol efficiently measuring the swelling rate of hydrogels. *MethodsX, 7*, Article 100779.

Zhang, L., Zhang, Q., Zheng, Y., He, Z., Guan, P., He, X., Hui, L., & Dai, Y. (2018). Study of Schiff base formation between dialdehyde cellulose and proteins, and its application for the deproteinization of crude polysaccharide extracts. *Industrial Crops and Products, 112*, 532–540.

Zhang, Z., Abidi, N., Lucia, L., Chabi, S., Denny, C. T., Parajuli, P., & Rumi, S. S. (2023). Cellulose/nanocellulose superabsorbent hydrogels as a sustainable platform for materials applications: A mini-review and perspective. *Carbohydrate Polymers, 299*, Article 120140.

Zheng, H., Mei, P., Wang, W., Yin, Y., Li, H., Zheng, M., Ou, X., & Cui, Z. (2023). Effects of super absorbent polymer on crop yield, water productivity and soil properties: A global meta-analysis. *Agricultural Water Management, 282*, Article 108290.